In situ surface/interface x-ray diffractometer for Oxide Molecular Beam Epitaxy

J. H. Lee[1,*], I. C. Tung[1,2], S.-H. Chang[3,**], Bhattacharya[3], D. D. Fong[3], J. W. Freeland[1], and Hawoong Hong[1,***]

[1]Advanced Photon Source, Argonne National Laboratory, Argonne, Illinois 60439, USA.

[2]Department of Materials Science and Engineering, Northwestern University, Evanston, Illinois 60208, USA.

[3]Materials Science Division, Argonne National Laboratory, Argonne, Illinois 60439, USA.

* The present address: Korean Atomic Energy Research Institute, 111 Daedeok-Daero, 989Beon-Gil, Yuseong-Gu, Daejeon, Korea.

** The present address: Department of Physics, Pukyung National University, 45 Yongso-Ro, Nam-Gu, Busan, Korea

** Corresponding author

In situ studies of oxide molecular beam epitaxy by synchrotron x-ray scattering has been made possible by upgrading an existing UHV/MBE six-circle diffractometer system. The existing main chamber was not changed and still has two separate sample positions, one for x-ray and one for electron diffraction. For oxide MBE growth, pure ozone delivery to the chamber has been made available, and several new deposition sources have been made available on a new 12" CF flange. X-ray diffraction has been used as a major probe for film growth and structures for the system. In

the original design, electron diffraction was intended for the secondary diagnostics available without the necessity of the x-ray. This concept runs against conventional MBE methodology. As a remedy, deposition of films was made possible at the above-mentioned positions. And, the aiming of the evaporation sources are fixed to the point between two locations. Ozone can be supplied through two separate nozzles for each location. Also two separate thickness monitors are installed. Additional features of the equipment are also presented together with the data taken during typical oxide film growth to illustrate the depth of information available via *in situ* x-ray techniques.

Research on complex oxide interfaces and superlattices is currently at the forefront of materials science and condensed matter physics [1]. Understanding the fundamental origins of the various exotic phenomena and novel electronic properties that appear in these materials will require the ability to probe and image the relevant interfacial structures in the growth environment, during and after deposition. Hard x-rays and diffraction techniques utilizing the high brightness of synchrotron-based light sources can greatly facilitate the study of such heterostructures, with sub-Ångstrom spatial resolution. We have previously built an instrument to conduct *in situ* studies of thin film growth, consisting a 6-circle diffractometer coupled to a UHV/molecular beam epitaxy (MBE) chamber [2]. This MBE diffractometer has been highly successful in the study of ultra-thin films, such as quantum well structures of metals on semiconductors and insulators [3,4]. In addition to investigating static ultra-thin film structures post-growth, we also performed 2-D mapping in reciprocal space in real time during film deposition [5-7]. To take advantage of recent trends in materials research toward complex oxides and their thin films, we extended our *in situ* synchrotron x-ray technique to the study of complex oxide deposition by oxide MBE, a fabrication technique that provides layer-by-layer control over the deposition processes.

The existing MBE diffractometer has been well described in the literature [2]. The existing chamber was designed mainly for the growth of metal-semiconductor systems, which allowed opportunities for the investigation of quantum well systems. However, for the possibility of future upgrades, the chamber was designed with multiple extra ports of various sizes; these extra ports ultimately facilitated the many changes and additions necessary for realizing an oxide-

MBE capability. Although a reflection high energy electron diffraction (RHEED) system was already part of the existing chamber, the growth processes were typically monitored with x-ray scattering, as the chamber permitted the observation of oscillations in the x-ray intensity, similar to RHEED oscillations, in real time. With the high brightness x-rays from the third generation synchrotrons and area detectors, 2-D scattering maps around the specular diffraction spot can be measured in real time. RHEED is used principally as a diagnostic for determining the smoothness and quality of the film, and its location is 8" inches away from x-ray diffraction position (Fig. 1). It is a challenge for conventional MBE users to adapt to new x-ray methods and combine x-ray diffraction capabilities with their MBE experience. They have been mostly depending on RHEED intensity oscillations to monitor and control the growth processes and parameters. More efforts will be required to establish correlations between x-ray and RHEED oscillations [8], and to develop x-ray specular/non-specular rod intensity distributions as intuitive indicators for the overall quality of films. We also anticipate x-ray surface diffraction images similar to RHEED images with high energy x-rays in the range of 100 keV [6].

The original chamber was intended for the growth of thin films with a small number of atomic layers. The chamber was equipped with only two ports for small evaporation sources. For larger capacity evaporation sources, new ports were added onto a large 12" CF flange (the multiport flange in Fig. 2-4). In traditional oxide-MBE, it is imperative to be able to monitor thin film growth with RHEED. However, the main advantage of our MBE-diffractometer is the ability to perform scattering with hard x-rays from the Advanced Photon Source. It was decided to maintain two different sample positions for deposition, one for *in situ* x-ray diffraction and the

other for RHEED measurements. However, as it would be difficult to alter the angle of the effusion cells to aim from one deposition point to another, a compromise was made such that the deposition sources are aimed at the midpoint between RHEED and x-ray diffraction position. This also required one additional thickness monitor and two ozone nozzles (see Fig. 3). The second thickness monitor is on a linear actuator and can be driven to the sample position for RHEED measurements or moved out of the way such that the sample holder can pass through the RHEED position and reach the sample transfer position.

To provide the necessary partial pressures of ozone near the face of the sample, a 1000 ltr/sec turbo pump was installed in addition to the existing ion pump and a titanium sublimation pump (Fig. 4). During oxide film growth, only the turbo pump is used. Nominally, 100% ozone is provided through an ozone distiller (DCA, Finland). The ozone pressure can be increased to reach a chamber pressure of 10^{-5} torr. Optionally, 10% ozone or pure oxygen can be supplied to the substrate through the ozone nozzles or to the whole chamber through a precision leak valve. The 12" CF multiport flange has been equipped with eight 2-3/4" CF ports out of which five aim at the midpoint between the x-ray diffraction position and the RHEED measurement position (Fig. 5). Among these five, the top one is a viewport and can be used to illuminate the inside of the chamber. Another port is aimed downward and is used for titanium sublimation. The remaining three ports are aimed upward and can be used for various effusion cells. Two ports are aimed at the x-ray position and have viewports installed. The last port is for an ozone nozzle and is aimed at the sample when it is at the RHEED location. A separate ozone nozzle is aimed toward the x-ray position using one of the spare ports on the main chamber. Each deposition

source has a pneumatic shutter consisting of a linear actuator (MDC) and a baffle made of Haynes Alloy 214. The sources are all equipped with water-cooled jackets and can be isolated from the main chamber with UHV mini-gate valves (VAT) to enable source reloading without having to vent the entire chamber. In addition, each cell can be pumped through a right angle valve on the cooling jacket independent of the main chamber so that the sources may be serviced without venting the main chamber.

For changing samples via the load lock, we employ Omicron-style sample plates and receivers. A wobble stick is used to pick up the sample plate from the sample dock and place it into the receiver. The receiver (Ferro-Vac, Switzerland) was originally developed for e-beam heating and has two spring-loaded sapphire balls that press down the sample plate against the receiver base to enhance the thermal conduction. For sample transfer, the sample holder must travel from the the x-ray position to ~2" beyond the RHEED position, toward the load lock (Fig.2). For this additional 2" motion of the sample, a new linear actuator was built to provide the extended sample motion. Originally the sample holder was equipped with multiple heating provisions: direct current through the substrate, radiative heating with a filament, and e-beam bombardment. The sample temperature could exceed 1200 °C. Although the previous sample holder had a flexible heating arrangement, the sample transfer mechanism was not implemented and the turnaround time for changing samples could take over 48 hours when including bake out and outgassing. With the new sample transfer and load-lock mechanism, the productivity of the MBE has been increased, and the turnaround time is now only a few hours. However, only one heating method is currently implemented. It is absolutely necessary to swap out substrates after each film

deposition to investigate film growth under different conditions. The new sample heating stage (Fig. 6) is based on a SiC (Morgan Advanced Material) element. Most of the parts of the heating stage are made of Haynes Alloy 214, which can withstand high temperatures and corrosive environments. The sample receiver and sample plates are also made of the same alloy. A heating power beyond 300W can be provided, and the sample temperature can reach 800 °C as measured by a pyrometer. Inside the heater housing, two layers of radiation shields (also Haynes Alloy 214) were installed. A thermocouple junction is located inside the housing next to the SiC element. This thermocouple does not touch the housing or the heating element.

The usual x-ray beam size is 0.5 mm or less in the horizontal direction (the vertical size is ~0.3 mm). As the sample temperature varies, there is some drift in the surface location. For precise alignment of the sample to the beam position, we added a motorized motion to the sample. The precision of the motion is 16 μm. This feature is important for the glancing angle diffraction geometry. The sample plate has an elevated platform (11 mm x 11 mm x 1mm) so that x-rays are not blocked by the receiver structure. The substrates are usually glued to the plate with silver paint and then heated in air to remove volatile substances from the paint. Welded clips can also be added to secure the sample to the plate. We use a mini-Ti ball (Agilent) as a Ti deposition source, and high temperature effusion cells (Veeco) with various crucibles and liners for the deposition of Co, Ni, La, and Fe. Dual filament cells (Veeco) are also available and have been used for Sr, Pb, Ba, Ca, and Bi deposition.

Time-resolved x-ray measurements can be performed at a Q corresponding to the anti-Bragg position on the specular rod. The oscillations in the x-ray intensities are similar to RHEED

intensity oscillation measurements in conventional MBE methods. Nowadays, 2-D detectors, such as the Pilatus-II (Dectris) pixel detector, are used for x-ray scattering measurements at synchrotron radiation sources. In typical film growth experiments, these detectors allow monitoring not only the scattered intensity at the anti-Bragg position but also the diffuse scattering around it. After the growth of a layer, we typically measure scattered intensity along the specular rod. This measurement is the same as a θ-2θ scan used in conventional film characterization. However, here the measurements are made *in situ*, and by exploiting a very large photon flux within a small beam size from undulator radiation, sub-Ångstrom length scale sensitivity can be easily achieved. This sensitivity to the initial interface formation and surface transformation of the first few atomic layers is crucial for understanding the mechanisms taking place during complex oxide thin film growth [9]. Data from typical film growth are presented in Fig. 7, which depicts time-resolved x-ray scattering during $LaCoO_3$ deposition onto $SrTiO_3$(001). Each column of pixels represents the scattered x-ray intensity distribution centered at **Q** = (0 0 0.5) in the reciprocal lattice units of $SrTiO_3$. Diffraction intensities were integrated along the rows of pixels in 2-D diffraction image. The pixel rows in the detector are positioned parallel to the film surface normal. Following the horizontal line of pixels along $Q_{//}$ (i.e., the momentum transfer parallel to the surface) = 0 in the 2-D data presentation, one can observe conventional x-ray intensity oscillations. The data shown here indicates layer-by-layer growth behavior. For $Q_{//} \neq 0$, the x-ray intensity comes from diffuse scattering, indicating island-island correlations [4, 10]. The satellites in the diffuse scattering moves closer to $Q_{//} = 0$ as the film growth proceeds, indicating that the island size is growing and the average distance between them is likewise increasing. The x-ray reflectivity data shown in Fig. 8 is a scan along the (0 0 L) specular direction. One can see distinct interference fringes coming from a 10-unit-cell-thick $LaCoO_3$

film. A more detailed analysis will be able to reveal the precise arrangement of atoms at the interface and the film [9].

We have described a new oxide MBE system for *in situ* x-ray diffraction, presenting the design concepts and capabilities, and given specific examples of utilization. This system will meet the requirements of the complex-oxide thin film community for extending and improving our understanding of interface formation and film structure evolution during growth.

The authors acknowledge discussions with D. G. Schlom, and S. A. Chambers. S.H.C., A.B. and D.D.F. were supported by the U.S. Department of Energy, Office of Science, Office of Basic Energy Sciences, Materials Sciences and Engineering Division. Work performed at Argonne National Laboratory, including the Advanced Photon Source, was supported by the US Department of Energy, Office of Science, Office of Basic Energy Sciences, under contract no. DE-AC02-06CH11357.

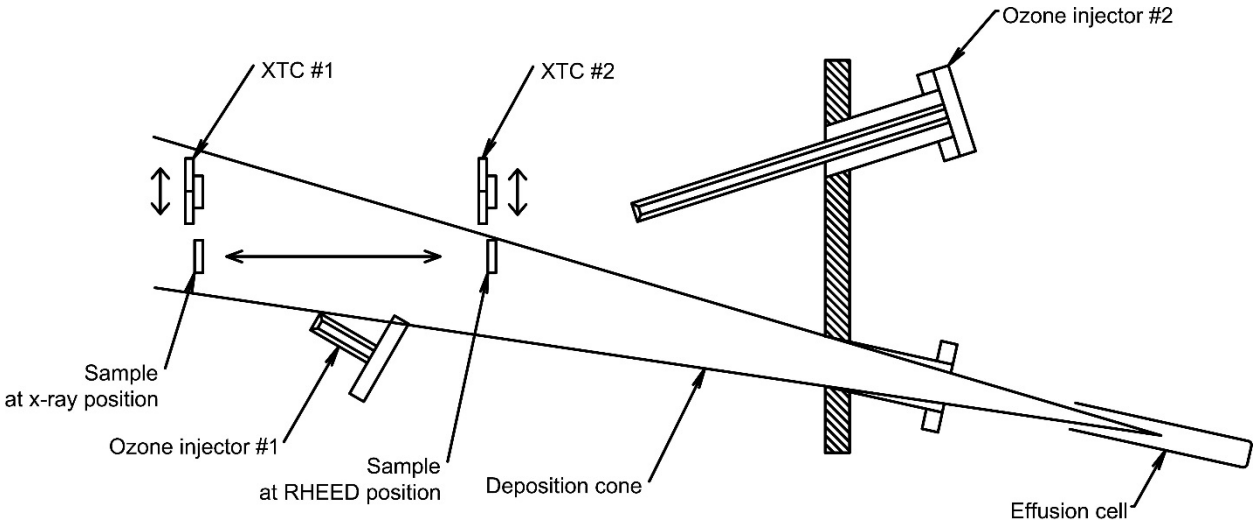

Fig. 1. The schematic drawing of the internal arrangements of sample positions for x-ray diffraction and RHEED. This is a composite cut-view from different cut direction for each component. The effusion cells and other deposition sources are aimed toward the midpoints between two sample positions. The thickness monitors (XTC #1 & #2) can be moved in and out of the sample position. Also the two ozone injectors are shown. The chamber walls are omitted for the clarity of the presentation.

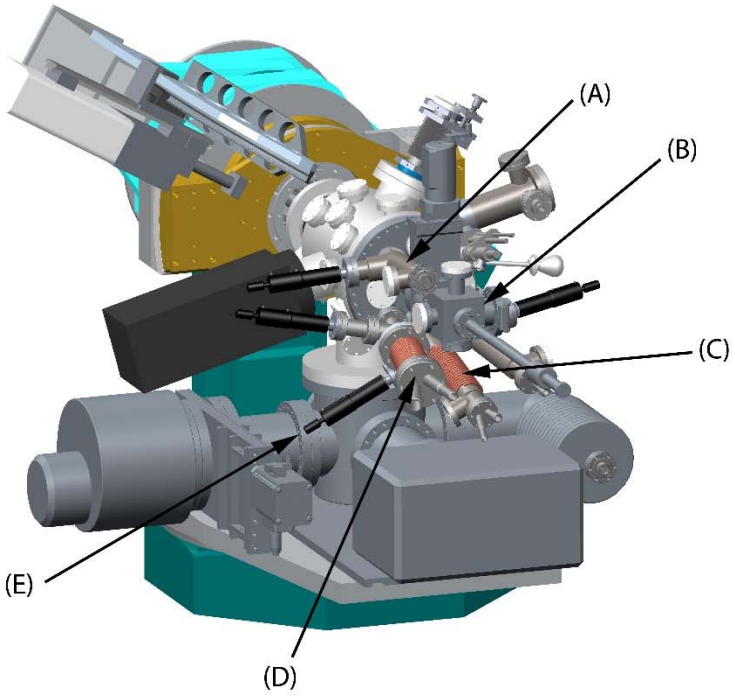

Fig. 2. The 3-D rendering of the design of oxide MBE capable 6 circle diffractometer. (A) A mini-Ti ball source. (B) The load-lock for sample transfer. (C) and (D) Effusion cells. (E) A shutter for effusion cells.

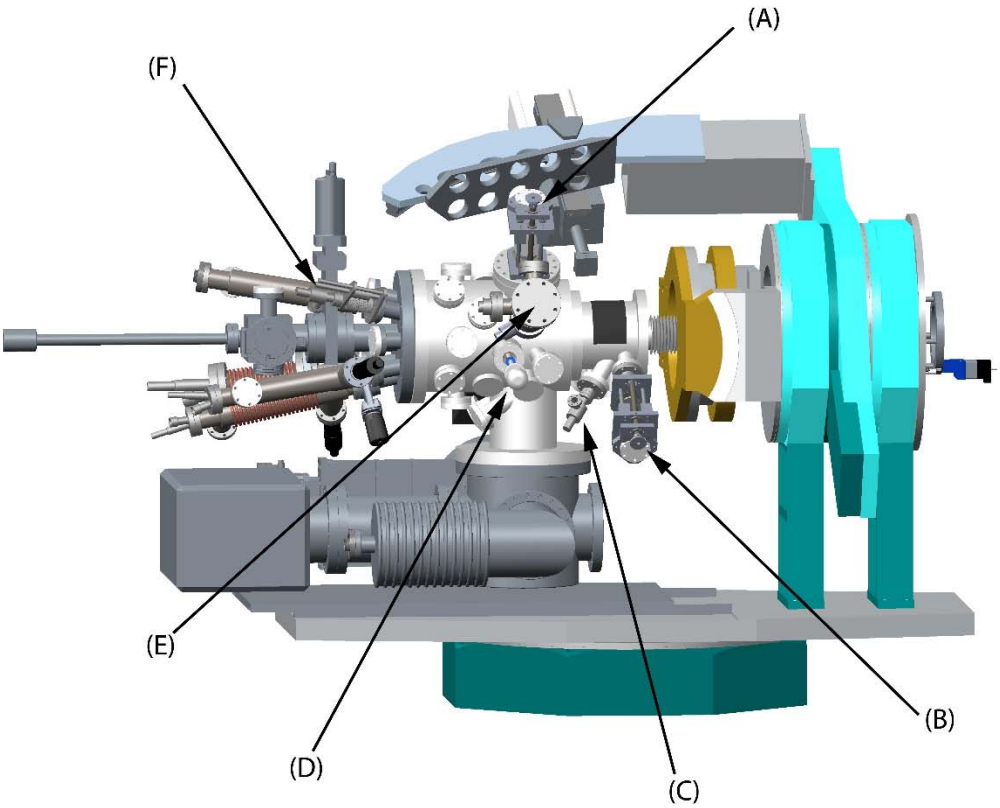

Fig. 3. The 3-D rendering of oxide MBE chamber on the 6-circle diffractometer: the upstream view. (A) Film thickness monitor #2. (B) Film thickness monitor #1. (C) Ozone injector #1. (D) Wobble stick. (E) RHEED gun. (F) Ozone injector #2.

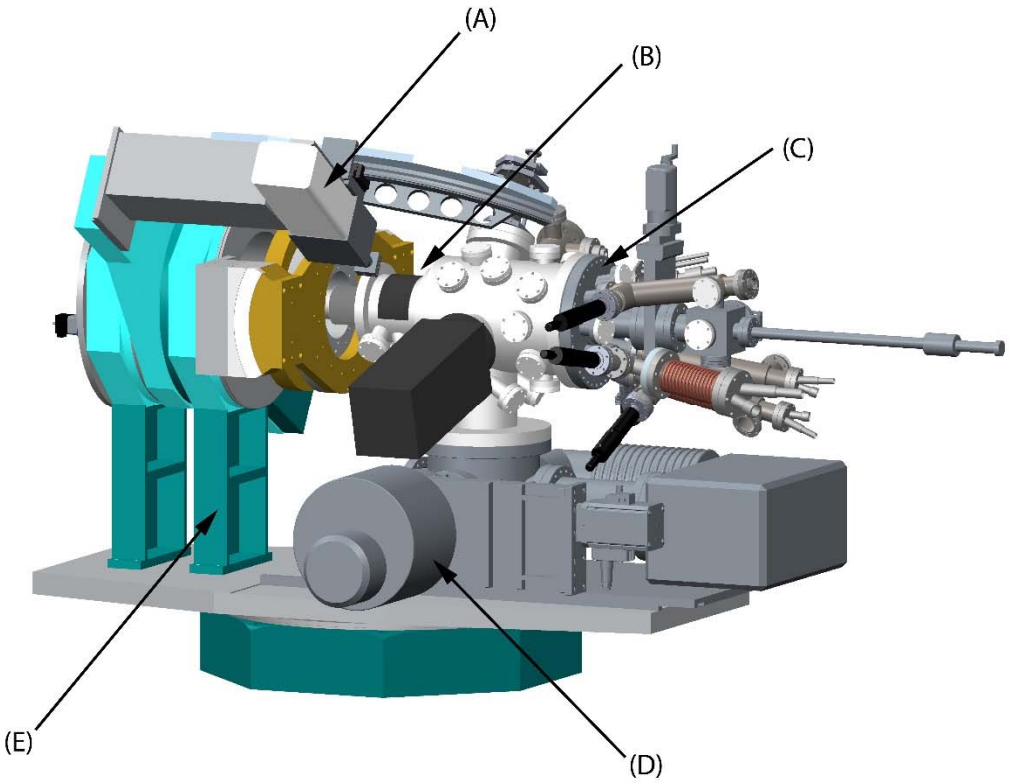

Fig. 4. The 3-D rendering of oxide MBE chamber on a 6-circle diffractometer: the downstream view. (A) X-ray detector. (B) Be window. (C) 12” multiport flange. (D) Turbo pump (1000 ltr/sec). (E) 6-circle diffractometer.

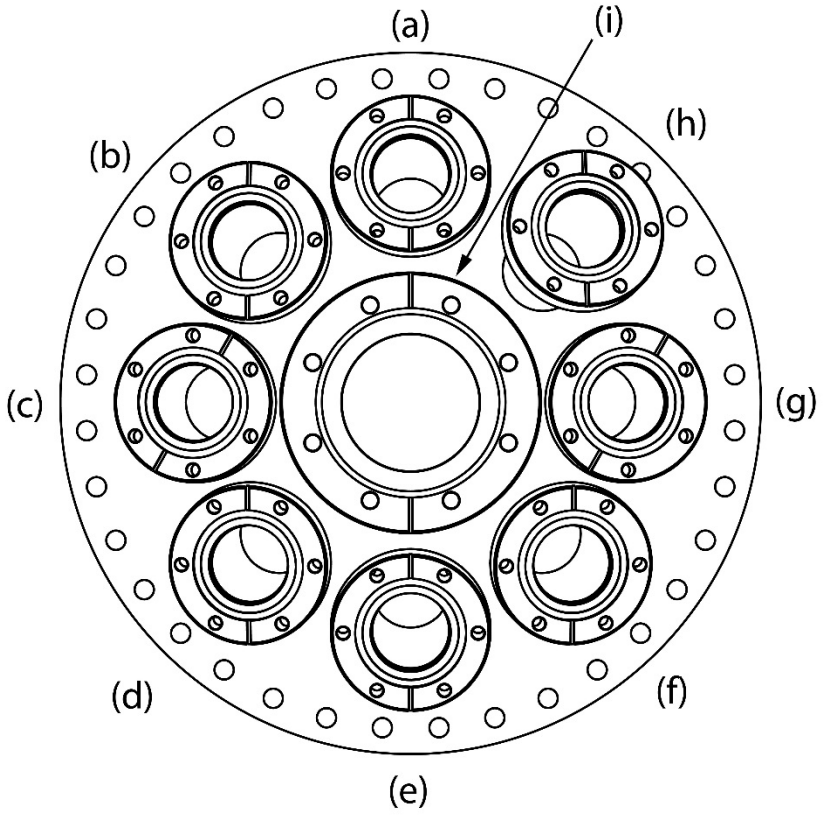

Fig. 5. Arrangement for ports on 12” multiport flange. Ports (a), (b), (d), (e), and (f) are aiming at the middle points between the x-ray diffraction and the RHEED positions. Ports (c) and (g) aim at the x-ray diffraction point. The port (h) aims at the RHEED position. (a) A viewport with a lamp. (b) A mini Ti-ball source. (c) and (g): viewports. (d), (e), and (f): effusion cells. (h) An ozone injector port. (i) A port for the load-lock.

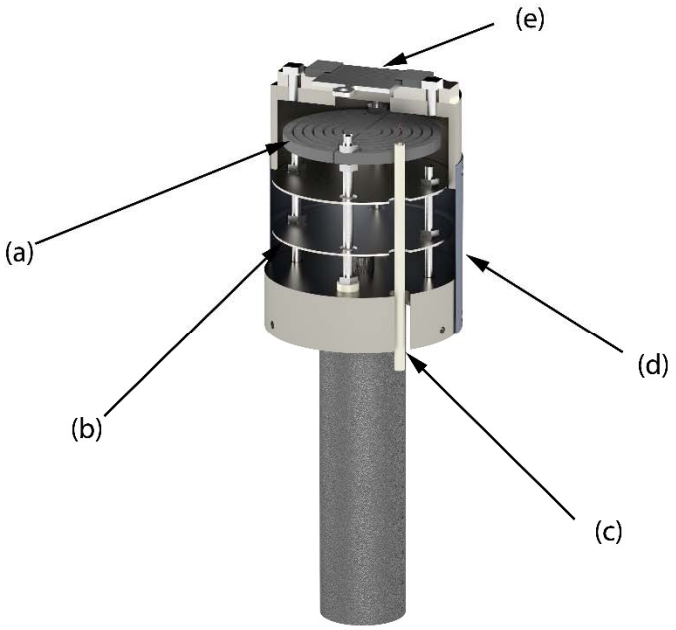

Fig. 6. The sample receiver and heating stage. (a) SiC heating element. (b) Radiation shields. (c) An alumina tube for a thermocouple (K-type). (d) Heater housing. (e) Sample platen and receiver.

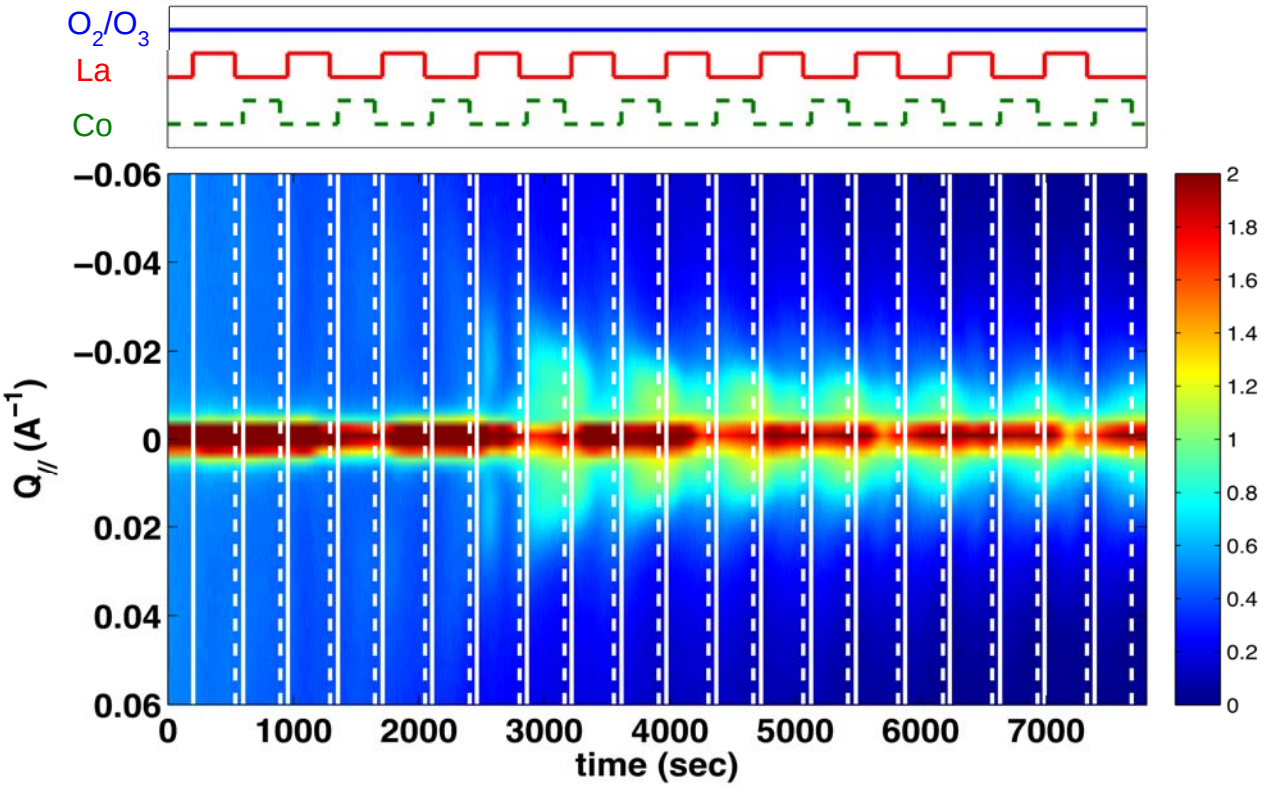

Fig. 7. Time dependent scattering during the sequential deposition of lanthanum and cobalt during the shuttered growth of 10 unit cell $LaCoO_3$. 10% ozone and molecular oxygen mixture is provided continuously during growth. Time-resolved x-ray scattering data shown in false color image. The diffuse scattering is the intensity projecting up and down from the line at $Q_{//} = 0$. The color bar on the right is shown in a logarithmic scale. The top graph shows the timing of shutters for La and Co sources and the ozone/oxygen mixture level.

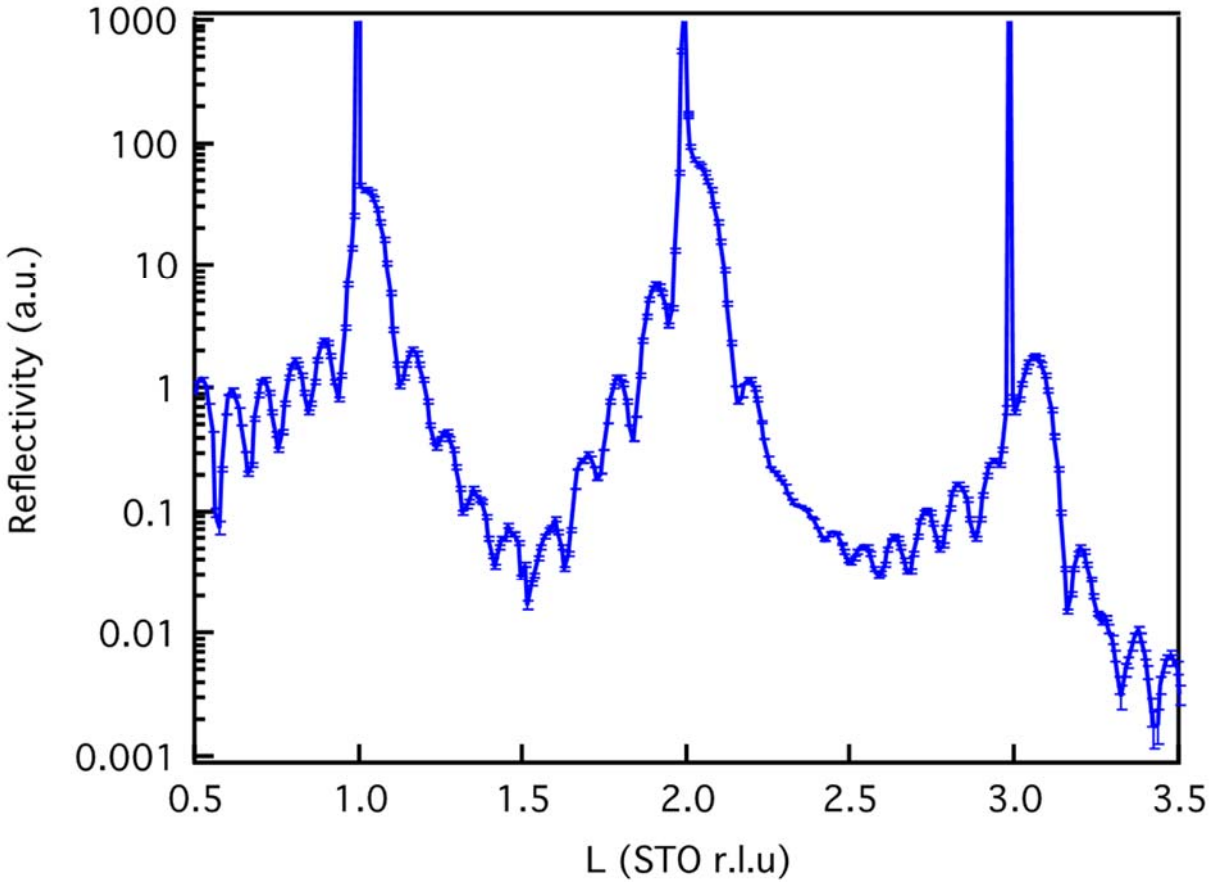

Fig. 8. X-ray reflectivity data with error bar from shuttered-growth LaCoO3 film (10ML) for scattering along the (00L) specular CTR.

References

1. J. Chakhalian, J. W. Freeland, A. J. Millis, C. Panagopoulos, J. M. Rondinelli, "Colloquium : Emergent properties in plane view: Strong correlations at oxide interfaces", Rev. Mod. Phys. **86**, 1189 (2014). A. Bhattacharya, S. J. May, "Magnetic oxide heterostructures", Annual Review of Materials Research **44**, 65 (2014).
2. Hawoong Hong, and T.-C. Chiang, "A Six-Circle Diffractometer Systems for Synchrotron X-ray Studies of Surfaces and Thin Film Growth by Molecular Beam Epitaxy," Nucl. Instr. and Meth. A **572**, 942 (2007).
3. P. Czoschke, H. Hong, L. Basile, and T.-C. Chiang, "Quantum beating patterns observed in the energetics of Pb film nanostructures," Phys. Rev. Lett. **93**, 036103 (2004).
4. Hawoong Hong, Aaron Gray, Ruqing Xu, Longxiang Zhang, and T.-C. Chiang, "Quantum Growth of a Metal/Insulator System: Lead on Sapphire" Appl. Phys. Lett. **97**, 241908 (2010).
5. Hawoong Hong, Z. Wu, T.-C. Chiang, P. Zschack, P. Jemian, H. Chen, and R.D. Aburano, "Reflection surface x-ray diffraction patterns: k-space images," Rev. Sci. Instrum. **71**, 3132 (2000).
6. Hawoong Hong, Aaron Gray, and T.-C. Chiang, "Real-Time Reciprocal Space Mapping of Nano-Islands Induced by Quantum Confinement", Metallurgical and Materials Transactions A **42**, 32 (2011).
7. Hawoong Hong, Z. Wu, T.-C. Chiang, P. Zschack, and H. Chen, "Time-resolved reflection surface x-ray diffraction," Rev. Sci. Instrum. **73**, 1720 (2002).
8. M. C. Sullivan M. J. Ward, Araceli Gutiérrez-Llorente, Eli R. Adler, H. Joress, A. Woll, and J. D. Brock, "Complex oxide growth using simultaneous *in situ* reflection high-

energy electron diffraction and x-ray reflectivity: When is one layer complete?", Appl. Phy. Lett. **106**, 031604 (2015)

9. J. H. Lee, G. Luo, I. C. Tung, S. H. Chang, Z. Luo, M. Malshe, M. Gadre, A. Bhattacharya, S. M. Nakhmanson, J. A. Eastman, H. Hong, J. Jellinek, D. Morgan, D. D. Fong, & J. W. Freeland, "Dynamic layer rearrangement during growth of layered oxide films by molecular beam epitaxy," Nature Materials **13**, 879–883 (2014).
10. J. Z. Tischler, G. Eres, B. C. Larson, C. M. Rouleau, P. Zschack, and D. H. Lowndes, Phys. Rev. Lett. **96**, 226104 (2006). J. D. Ferguson, G. Arikan, D. S. Dale, A. R. Woll, and J. D. Brock, "Measurements of Surface Diffusivity and Coarsening during Pulsed Laser Deposition", Phys. Rev. Lett. **103**, 256103 (2009).